ASYMMETRIC VARIATIONS OF THE CORONAL GREEN LINE INTENSITY

V. P. TRITAKIS[1], H. MAVROMICHALAKI[2], and B. PETROPOULOS[1]

(Received 5 August, 1987; in revised form 18 February, 1988)

Abstract. The analysis of the daily measurements of the coronal green line intensity, which have been extensively tested for homogeneity and freedom of trends observed at the Pic-du-Midi observatory during the period 1944–1974, has revealed some characteristic asymmetric variations. A north–south asymmetry of the green line intensity is the main feature of the period 1949–1971 while a south–north one is obvious within 1972–1974 and the minor statistical significance span 1944–1948. On the other hand a significant W–E asymmetry has been confirmed in the whole period 1944–1974. It is noteworthy that the period 1949–1971, where the N–S asymmetry takes place consists a 22-yr solar cycle which starts from the epoch of the solar magnetic field inversion of the solar cycle No. 18 and terminates in the relevant epoch of the cycle No. 20.

The combination of N–S and S–N asymmetry with a W–E one makes the NW solar-quarter to appear as the most active of all in the 22-yr cycle 1949–1971, while in the periods 1944–1948 and 1972–1974 the SW quarter is the most active. Finally, from the polar distribution of the green line intensity has been derived that the maximum values of the asymmetries occur in heliocentric sectors $\pm 10°$–$20°$ far from the solar equator on both sides of the central meridian.

Physical mechanisms which could contribute to the creation of both N–S and E–W asymmetries of the solar activity and the green line intensity as an accompanied event, like different starting time of an 11-yr solar cycle in the two solar hemispheres, the motion of the Sun towards the Apex, and short-lived 'active' solar longitudes formed by temporal clustering of solar active centers, have been discussed.

1. Introduction

The extremely high temperature of the solar corona causes line radiation from highly ionized atoms the most important of which are in the visible wavelengths, the red (Fe X λ6374 Å), the green (Fe XIV λ5303 Å) and the yellow (Ca XV λ5694 Å) lines.

Visual observations of the green line collected by a Lyot-type coronagraph and spectrograph during three solar cycles have revealed an extremely inhomogeneous corona with both low density regions known as 'coronal holes' where the green line intensity is especially weak (Waldmeier, 1981) and high density areas where the intensity increases (Leroy and Trellis, 1974). Useful information about the intensity of this line can be inferred by detailed observations of the electron density within coronal holes and dense coronal regions (Noëns and Leroy, 1981).

The green line intensity has been studied extensively in relation to various solar, interplanetary, and geophysical parameters while quantitative models have been presented.

Some interesting correlations of the green line intensity with sector boundaries of the

[1] Research Center for Astronomy and Applied Mathematics, Academy of Athens, Athens GR 10673, Greece

[2] Physics Department, Nuclear Physics Section, University of Athens, Athens 10680, Greece.

Solar Physics **115** (1988) 367–384.

heliospheric current sheet and the solar wind velocity have been reported by Antonucci (1974) and Pathak (1971), respectively. On the other hand Stenflo (1972), bearing in mind that the intensity of the green line increases with coronal temperature found that the latitudinal distribution of the green line intensity follows closely that of sunspots, the faculae and the strength of magnetic fields. Quantitative expressions of the green line intensity in relation to sunspots, faculae, the number of proton flares and the red emission line at 6374 Å have been also presented by Waldmeier (1971), Cuperman and Sternlieb (1972), Xanthakis, Petropoulos, and Mavromichalaki (1980, 1981).

Two prominent maxima of the green line intensity in every solar cycle have been denoted by Pathak (1972), while Xanthakis, Petropoulos, and Mavromichalaki (1981) have pointed out that the green line intensity can be considered as an integrated index of the solar activity.

One of the most interesting feature of the green line intensity is a north–south asymmetry which shows a negative correlation with the solar activity in the sense that it is small in the maxima and high in the minima (Pathak, 1972; Rušin, 1980). In the opposite, some investigations for a possible E–W asymmetry of the green line intensity or other solar activity manifestations were not able to come to significant conclusions (Růžičková-Topolová, 1974; Letfus and Růžičková-Topolová, 1980).

In the present study we analyze a long time series of green line intensity values which has been derived to be adequately homogeneous and reliable (see next paragraph), intending to result to confident conclusions about possible asymmetries of this line.

2. Data

Daily measurements of the absolute intensity of the coronal emission line 5303 Å taken from the Pic-du-Midi Observatory for the period 1944–1974 were used in this work.

These measurements have been obtained by a classic Lyot-type coronagraph for all heliocentric sectors around the solar limb with a resolution of 5° and a distance of about 40″ until 2″ from the Sun's edge. Hence, our data are obtained in a polar coordinate system defined by the central meridian passage. The unit of the measured intensity of this line is 10^{-6} times the intensity at a width 1 Å wavelength of the continuous photospheric spectrum (Rozelot and Fulconis, 1983; Dollfus, 1971). From the daily measurements of the green line intensity, yearly mean values in each heliocentric sector and in each north, south, east, west solar hemisphere have been calculated.

The number of days when observations have been obtained as well as the number of months where these measurements are distributed, have been entered in Table I. From the entries of this table, it is evident that the data of the years 1944 and 1945 do not offer sufficient statistical confidence because the mean values of these years have been calculated by 12 and 37 daily observations, respectively, which are distributed in only two months for each year.

In the opposite the measurements after 1971 are less significant than those of the previous years (1946–1971) but they do not lose their statistical confidence because they are distributed in 10–11 months for each year making a reliable representation of the

TABLE I

Green coronal line coefficients of asymmetry and data sample parameters

Year	Months per year	Daily observations per year	Yearly N–S asymmetry coefficient (%)	Yearly E–W asymmetry coefficient (%)
1944	2	12	0.06	−0.33
1945	2	37	−0.26	−0.11
1946	8	52	0.10	0.02
1947	12	91	−0.04	0.02
1948	11	112	−0.08	0.01
1949	12	125	0.08	−0.05
1950	12	145	0.16	−0.06
1951	12	111	0.13	−0.10
1952	12	106	0.09	−0.12
1953	12	139	0.15	−0.09
1954	12	137	0.06	−0.04
1955	12	149	0.15	−0.05
1956	12	186	0.09	−0.16
1957	12	152	−0.09	−0.09
1958	12	137	0.06	−0.14
1959	12	161	0.12	−0.10
1960	11	105	0.18	−0.03
1961	12	143	0.16	−0.09
1962	11	111	0.21	−0.10
1963	11	108	0.22	−0.05
1964	12	132	0.22	−0.06
1965	12	123	0.28	−0.09
1966	12	141	0.43	−0.06
1967	12	144	0.16	−0.06
1968	12	122	0.04	−0.04
1969	11	127	0.06	−0.09
1970	12	133	0.10	−0.06
1971	9	71	0.09	−0.07
1972	12	79	−0.08	−0.10
1973	10	61	−0.01	−0.08
1974	10	41	−0.25	−0.11

corresponding year. The yearly values of the period 1946–1974 have been calculated by samples of daily observations the sizes of which vary from 41 to 186 (Table I).

These sample sizes represent less than 50% of the data population of a certain year (size $N = 365$), hence serious doubts could be arised about the validity of the data set we use in the present paper. For this reason it is fair to check these data with suitable tests of significance giving confidence limits at which we can trust results derived by this set. The time series under consideration contains mean yearly values of the green line intensity within each solar quarter for the period 1946–1974, namely our data set contains 4 values per year × 29 years = 116 values.

At the beginning, we separate the total record of data in four successive subrecords

with sizes $N = 29$. Significant differences between these subrecords can be detected by a Student's t-test the equation of which states

$$t_{dk,k+1} = \frac{\bar{x}_k - \bar{x}_{k+1}}{\left[\frac{N_k S_k^2 + N_{k+1} S_{k+1}^2}{N_k + N_{k+1} - 2}\left(\frac{1}{N_k} + \frac{1}{N_{k+1}}\right)\right]^{1/2}}, \tag{1}$$

where $\bar{x}_k$, $\bar{S}_k$, N_k are the mean, the standard deviation, and the size of a certain subrecord k ($k = 1, 2, 3$), respectively. Actually, we test the hypothesis H_0 that all the subrecords come from the same population of data against the hypothesis H_1 that they do not. In essence we wish to decide between the hypotheses $H_0: \bar{x}_k = \bar{x}_{k+1}$, $k = 1, 2, 3$ namely, all the subrecords belong to the same population of data, and $H_1: \bar{x}_k \neq \bar{x}_{k+1}$, $k = 1, 2, 3$ which implies that significant differences exist among the subrecords that is, they belong to various populations (Kendall and Stuart, 1966).

The application of the relation (1) to the statistics of the subrecords of our data set has given the following t-scores:

$$t_{d_{1,2}} = 0,2\,, \qquad t_{d_{2,3}} = 0,6\,, \qquad t_{d_{3,4}} = -1,3\,.$$

For a two-tailed t-test at a 0.01 level of significance we adopt the following decision rules:

(a) Accept H_0 if $t_{dk,k+1}$ stays within the range $\pm t_{0.995}$, namely $-t_{0.995} < t_{dk,k+1} < +t_{0.995}$.

(b) Reject H_0 otherwise.

From a t-distribution table we find for $V = N_1 + N_2 - 2 = 2N - 2 = 2 \times 29 - 2 = 56$ deg of freedom that $t_{0.995} \approx 3$. Since all the $t_{dk,k+1}$ values presented above complete the rule (a), we accept the H_0 hypothesis that the subrecords of the data under consideration belong to the same population of data. In essence, the results of this test imply that our data set presents a remarkable homogeneity significant at a 0.01 confidence level.

In the following, we proceed to additional statistical tests which examine if our data are free of trends which may introduce asymmetries without physical meanings. For this purpose we apply a Mann–Kendall's rank test the t_{MK}-score of which is defined by the relation

$$t_{\mathrm{MK}} = \frac{4P}{N(N-1)} - 1\,, \tag{2}$$

where $P = \Sigma_l^{N-l} n_i$, n_i being the number of latter terms whose values exceed the consecutive values of the data record, and $N = 116$ the record size (Kendall, 1948). For $N \geq 10$, the statistic t_{MK} is nearly Gaussian with zero expectation value and variance equal to $(4N + 10)/9N(N - 1)$ so that it can be tested for its statistical significance.

The application of the relation (2) for the data under consideration gave $t_{\mathrm{MK}} = 0.03$

while the critical value $t_{0.01}$ can be calculated by the relation

$$t_{0.01} = t_{st} \sqrt{\frac{4N + 10}{9N(N - 1)}} , \tag{3}$$

where t_{st} the value we get from the table of the percentile values for Student's t-distribution for 0.01 confidence level and $N - 1$ degrees of freedom (Mitchell, 1963).

Finally, the value we get from the relation (3) is $t_{0.01} = 0.164$ and obviously $t_{MK} (= 0.03) < t_{0.01} (= 0.164)$ fact which implies that our data set is free from trend at a 0.01 confidence level at least.

The absence of trend in our time series is supported by the small slope of the regression line of the data defined by the relation

$$Y = 0.03t + 29.68 ,$$

where Y the data values and t the time in years.

Closing this paragraph, it is fair to say that the data set we use in this report is consistent to a homogeneous and free of trend time-series.

3. Latitudinal Asymmetry of the Green Line Intensity

A common way to express asymmetries is the asymmetry coefficient

$$A = \frac{N - S}{N + S} ,$$

where in our case N, S are mean yearly values of the green line intensity in the north and south solar hemisphere, respectively.

In Figure 1 the yearly variation of the north–south (N–S) (Figure 1(a)), northwest–southwest (NW–SW) (Figure 1(b)), northeast–southeast (NE–SE) (Figure 1(c)) asymmetry coefficient for the time span 1944–1974 is depicted. From Figure 1(a) it is apparent that the variation of the north–south asymmetry coefficient confirms the conclusions of previous papers that the integrated green line intensity in the north solar hemisphere appears in general more intensive than the south and that the maximum asymmetry of this coefficient appears in the year 1966. It is also confirmed that after 1971 the north–south asymmetry has the tendency to turn to south–north. The dotted line in Figure 1(a) represents the coefficient $\Sigma H_N - \Sigma H_S / \Sigma H_N + \Sigma H_S$ where ΣH_N, ΣH_S are the annual sums of the maximum values of the sunspot magnetic field intensity observed for each group of sunspots during each passage of it over the visible solar hemisphere. These data have been compiled in the Mount Wilson Observatory and extend to the time span 1917–1958 (Xanthakis, 1967). From the Figure 1(a) it is evident that there is a close covariance between the north–south asymmetries of the coronal green line intensity and the solar magnetic field which implies that a close correlation between the green line intensity and the solar activity must be expected. The correlation coefficient between the north–south asymmetries of the green line intensity $\Delta I_{N,S}$ and

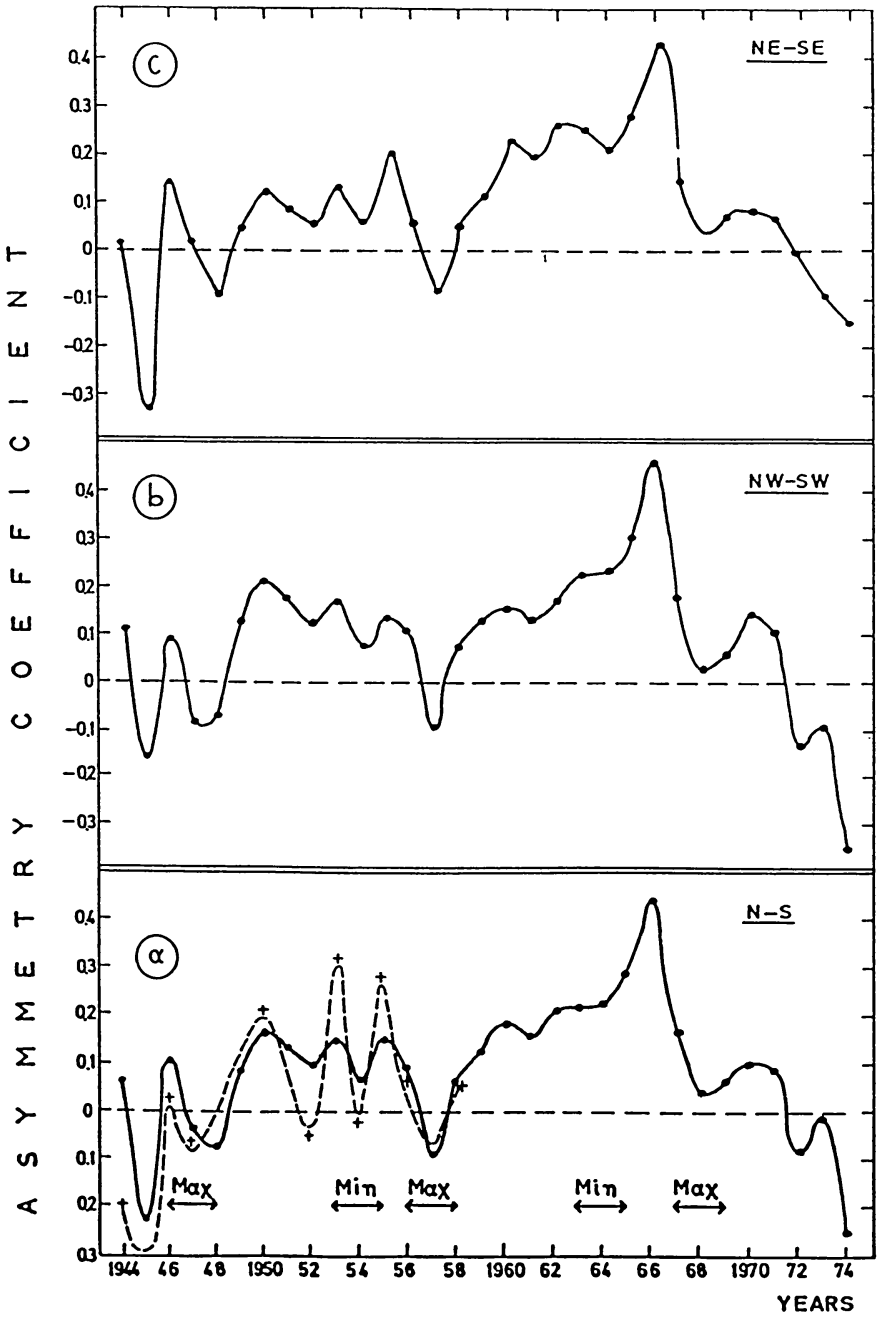

Fig. 1. Variations of the north–south (lower panel) northwest–southwest (intermediate panel), and northeast–southeast (upper panel) asymmetry coefficient in the time period 1944–1974. The dotted line in the lower panel represents the variation of the asymmetry coefficient of the sums of the maximum values of the sunspot magnetic field intensity observed for each group of sunspots during each passage of it over the visible solar hemisphere, Max and Min denote the epochs of extrema of the 11-yr cycles No. 18–20.

the maximum values of the sunspot magnetic field intensity $\Delta\Sigma H_{N,S}$ as well as the relevant coefficients between the green line intensity and the maximum magnetic field in the total solar disc, in the north and the south solar hemispheres, namely the coefficients between the variables. $(I_{\text{tot}}, \Sigma H_{\text{tot}})$, $(I_N, \Sigma H_N)$, $(I_S, \Sigma H_S)$ have been tabu-

TABLE II

Correlation coefficients between the green line intensity and the maximum values of the solar magnetic field intensity

Variables	Correlation coefficients	Level of significance ($N = 15$)
$\Delta I_{N,S}, \Delta \Sigma H_{N,S}$	0.80	0.001
$I_{tot}, \Sigma H_N$	0.88	0.001
$I_N, \Sigma H_N$	0.86	0.001
$I_S, \Sigma H_S$	0.78	0.001

lated in Table II. These coefficients are not extremely high but they are statistically significant for the concrete sample size ($N = 15$) at a 0.01 confidence level. Hence, a possible correlation between the green line emission and the small scale solar magnetic fields is denoted. An additional information of Figure 1(a) is that the north–south asymmetry around the maxima of the solar cycles Nos. 18, 19 (years 1947, 1957) turns to negative while in the maximum of the cycle No. 20 it is positive showing in this way a 22-yr feature of the green line asymmetry in the epoches of maxima. Closing the description of Figure 1 we underline that all the panels of Figure 1 are the same in structure and in order of magnitude, fact which argues that the north–south asymmetry is homogeneously distributed in the direction of the solar equator in the sense that there is no significant difference between the NE–SE and the NW–SW asymmetry.

North–south asymmetries have been detected in most of the solar activity manifestations, like sunspot numbers (Swinson, Koyama, and Saito, 1986), solar flares (Roy, 1977), photospheric magnetic fields (Howard, 1974), interplanetary magnetic sector structure (Tritakis, 1984), etc., so a N–S asymmetry of the green line intensity described above probably reflects a unique solar activity unevenness. Temporal and spatial variations of the solar differential rotation, which might be evidences of large-scale kinematics in the solar interior (Eddy, 1976) are probably major reasons of the formation of the N–S asymmetry of the solar activity. Differences in the starting time and the evolution of the solar cycle in the two solar hemispheres of the order of 1–2 years which support this aspect and they could explain to some extend N–S asymmetries have been detected by Bumba and Howard (1969).

Closing this paragraph, we present a Blackman–Tuckey power spectrum of the quarterly values of the latitudinal asymmetry coefficient of the green line intensity which exhibits a peak (lag = 18) significant at 0.05 confidence level corresponding to a period of about 3.6 quarters or 3.6 quarters × 3 months/quarter ≈ 11 months (Figure 2). Since the data we analyse in this report have been pointed out to be free from trends or irregularities this almost yearly periodicity of the N–S asymmetry of the green line intensity must be a real one corresponding to temporal variations of the asymmetry of the solar activity in the two solar hemispheres.

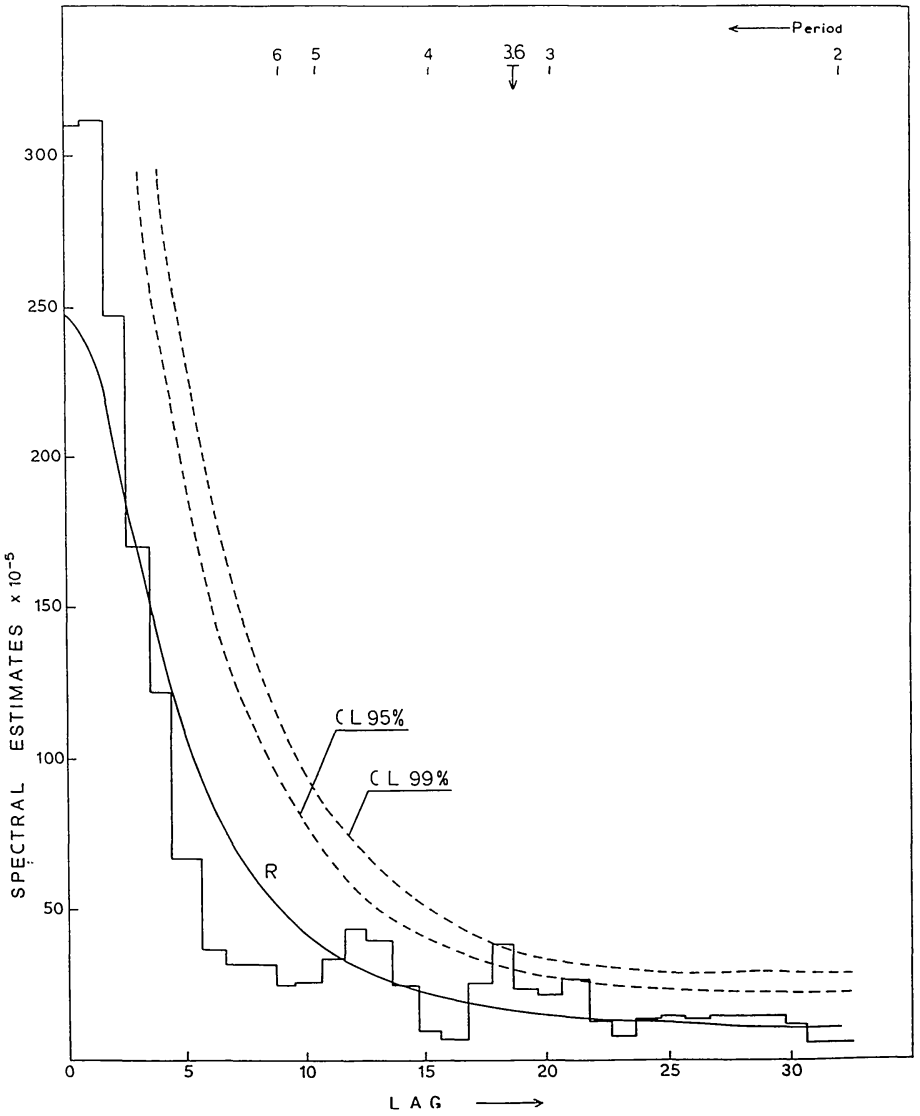

Fig. 2. Blackman–Tuckey power spectrum of the N–S asymmetry coefficient of the green line intensity. The significance of the deviation of the outstanding peaks from the Markov red noise (R) can be evaluated by means of the confidence level curves CL.

4. Longitudinal Asymmetry of the Green Line Intensity

In Figure 3 the yearly variation of the east–west (E–W) (Figure 3(a)), northeast–northwest (NE–NW) (Figure 3(b)) and southeast–southwest (SE–SW) (Figure 3(c)) asymmetry coefficient for the time span 1945–1974 is depicted.

From this figure, it is clear that the green line intensity predominates in the west solar hemisphere for the whole period 1944–1974. Figures 3(b) and 3(c) are similar to Figure 3(a) but they contain interesting characteristics which deserve additional description. Figure 3(c) is almost the same with Figure 3(a) but after 1971 the asymmetry variation follows a descending march which evidently corresponds to the N–S asymmetry inversion which has been determined in Figure 1. The descending march of the SE–SW asymmetry after 1971 reveals that the N–S asymmetry inversion to S–N starts

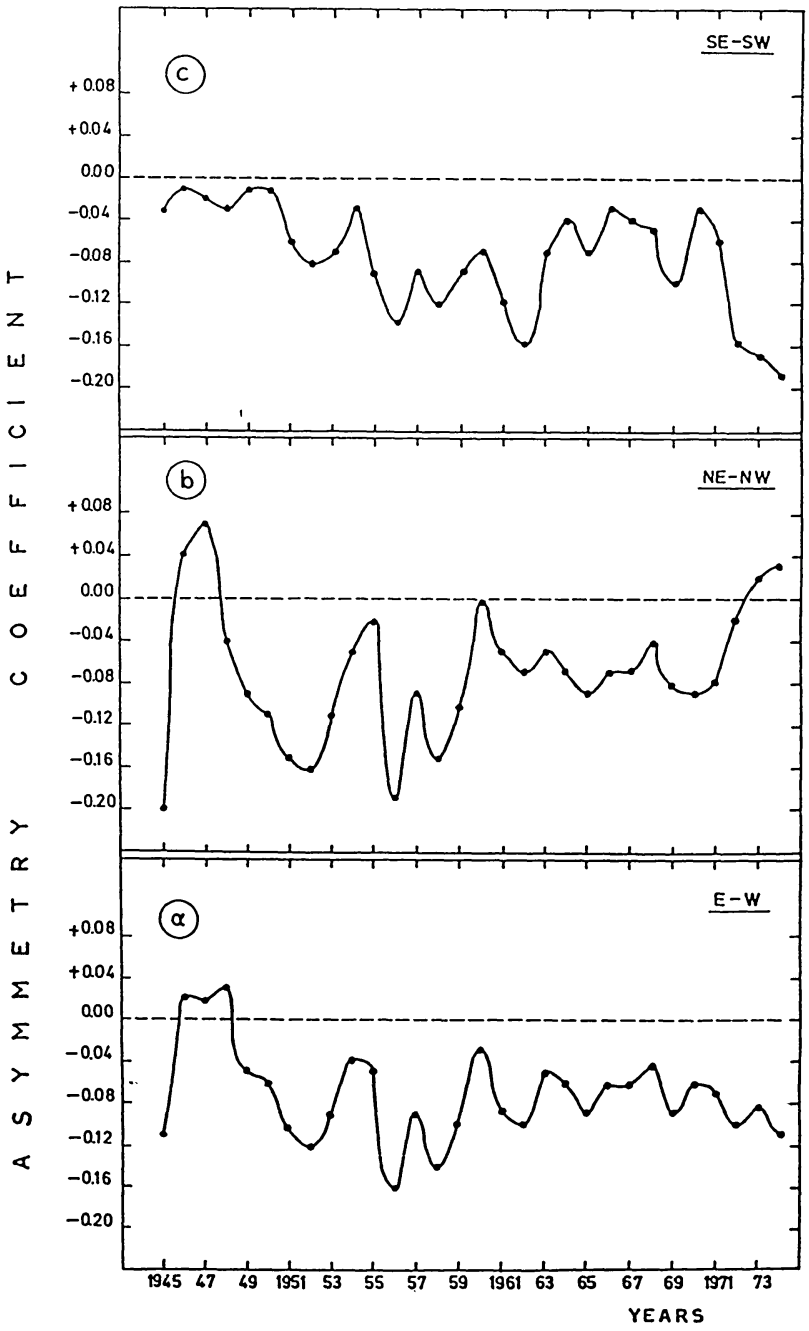

Fig. 3. Variations of the east–west (lower panel), northeast–northwest (intermediate panel) and southeast–southwest (upper panel) asymmetry coefficient in the time period 1944–1974.

in the SW solar quarter. Comparison of Figures 3(a), 3(b), 3(c) shows that the contribution of the NE–NW asymmetry (Figure 3(b)) in the final formulation of the E–W asymmetry (Figure 3(a)) is more significant than the SE–SW one (Figure 3(c)). In most of the cases the NE–NW asymmetry reaches higher absolute values than those of the SE–SW fact which probably implies that the NW solar quarter is more active than the SW in the span 1944–1971.

After the year 1971 excessive activity seems to be transferred to the SW quarter which

is illustrated by the rapid increase of the NE–NW variation and which finally causes the inversion of the N–S asymmetry to S–N.

Figure 4 represents the variation of the NE–SW (Figure 4(a)) and the NW–SE (Figure 4(b)) asymmetry, namely the asymmetries among the four solar quarters crosswise. Figure 4(a) looks alike with Figure 1(a, b, c) but the high negative values of the NE–SW after 1971 argue for the predominance of the SW solar quarter and its contribution to the N–S to S–N asymmetry inversion. On the other hand, from Figure 3(b) it is obvious that the NW–SE asymmetry is positive within the most of the period 1944–1974, thus it is confirmed that the NW solar quarter predominates on the SE one.

In the following we mention the most interesting east–west asymmetries which have

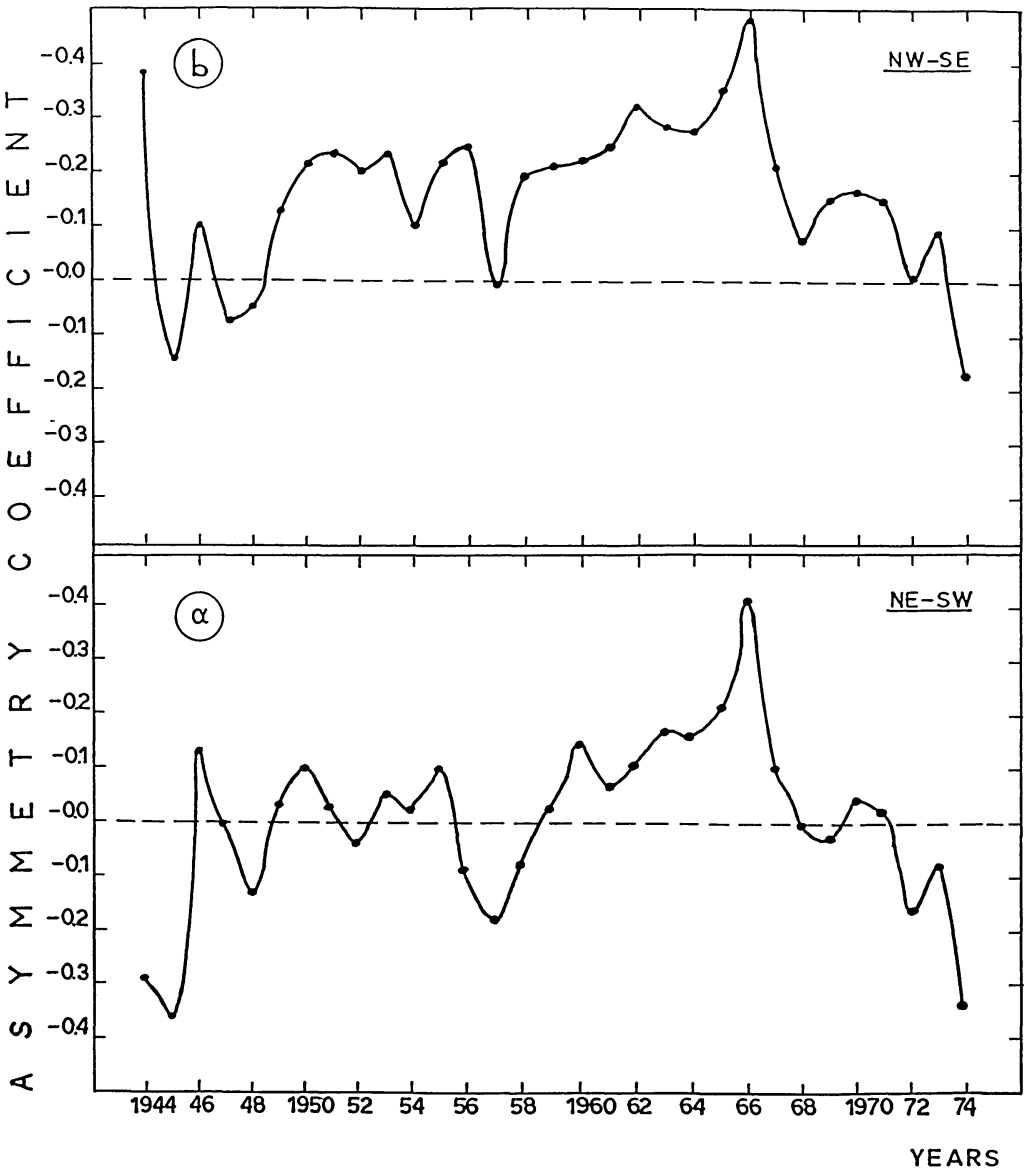

Fig. 4. Variations of the northeast–southwest (lower panel) northwest–southeast (upper panel) asymmetry coefficient in the time period 1944–1974.

been reported in various solar events, though this unevenness it is not easily understood. A slight E–W asymmetry of the total spot areas had been mentioned at first since the beginning of our century but it was explained as a rather figurative effect (Maunder, 1907). Finally it was explained as the result of a positive radial gradient of angular rotation in the Sun which caused the vertical axis of a sunspot to be tilted westwards on the average by a half degree. That tilt foreshortened the spots, thus systematically decreasing their apparent areas, but more in the western than in the eastern half of the disk (Minnaert, 1946). A longitudinal asymmetry of the solar activity together with a latitudinal one arised by a paper of Bumba and Howard (1969) while an E–W asymmetry in the solar flares distribution have been reported by Letfus and Růžičková-Topolová (1980) and Jin, Zhao, and Fu (1986).

An idea of explaining the E–W asymmetry of solar activity phenomena considers the effect of an external influence on solar activity, associated with the motion of the Sun towards the Apex. Trellis (1960) has reported that the green coronal line is brighter in the solar region facing the Apex and the red line is fainter. In addition, more active regions seemed to be born at heliocentric longitudes facing the Apex as consequence of asymmetry in the structure of the electromagnetic fields due to the motion of the Sun toward the Apex (Trellis, 1967). If this motion has really some influence on the behaviour of the solar activity we would expect:

(1) a variation with heliographic latitude of the N–S asymmetry;

(2) a variation during the year of the E–W asymmetry (Cantú, Godoli, and Poletto, 1970).

As far as point (1) is concerned a significant variation of the green line intensity with heliographic latitude has been detected by Moussas *et al.* (1982) which could confirm to some extend this point.

Concerning to point (2), the evaluation of a yearly variation of the E–W asymmetry is not very simple. In Figure 5 a Blackman–Tuckey power spectrum of the quarterly values of the E–W asymmetry of the green line intensity shows significant peaks, at 0.05 confidence level, which correspond to periods of 4 and 30 quarters (lags 15 and 2, respectively) namely to $4 \times 3 = 12$ months and $30 \times 3 = 90$ months = 7.5 years. The long periodicity of 7.5 years has probably to do something with the first harmonic of a 16–17-yr evolution of activity in the solar corona which has been detected by Leroy and Noëns (1983) during the analysis of the same data we are analysing in the present article. As far as to the yearly periodicity which corresponds to the lag 15 at first glance it seems to support point (2). However, at the end of June the Sun–Earth line passes by the Apex so we expect a yearly variation of the asymmetry which is higher in the second half than the first of a year.

In Figure 6 we represent the semi-annual values of the E–W asymmetry coefficient of the green line intensity in the time period 1947–1973. From this figure it is evident that the values of the second semester of the year (dashed line) are greater in most of the cases than those of the first semester (continuous line). Actually semi-annual E–W asymmetry values of the second semester fail to be greater than those of the first semester in nine cases (encircled points on Figure 6) while they are clearly greater in the rest

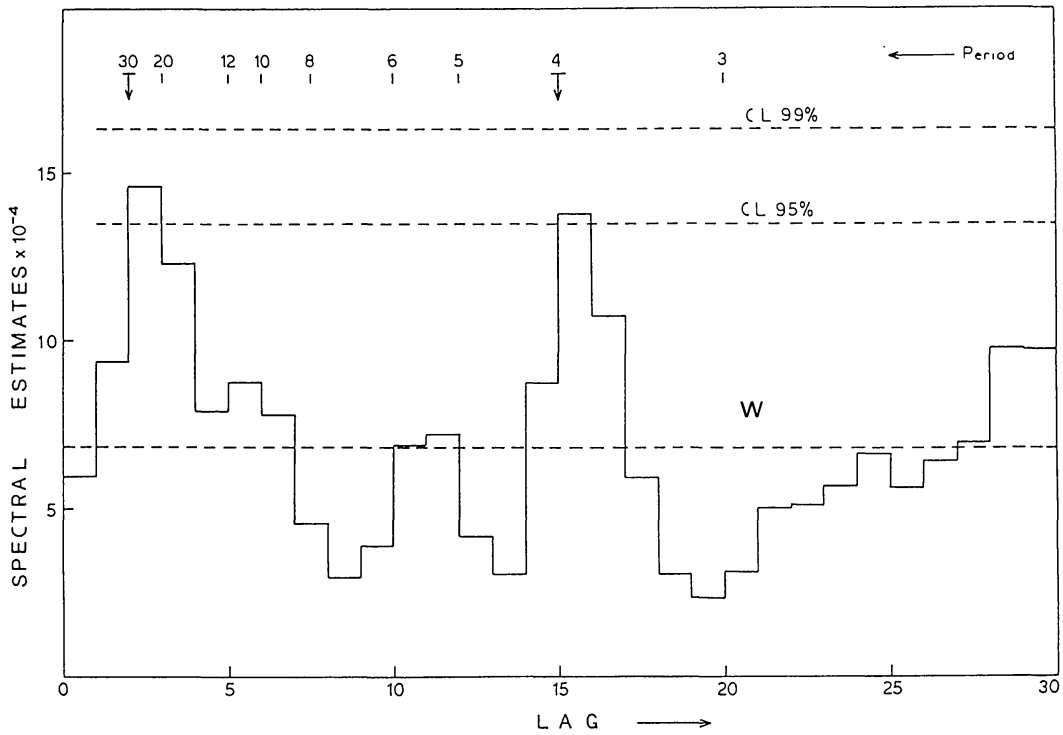

Fig. 5. Blackman–Tuckey power spectrum of the E–W asymmetry coefficient of the green line intensity. The significance of the deviation of the outstanding peaks from the white noise (W) can be evaluated by means of the confidence level curves CL.

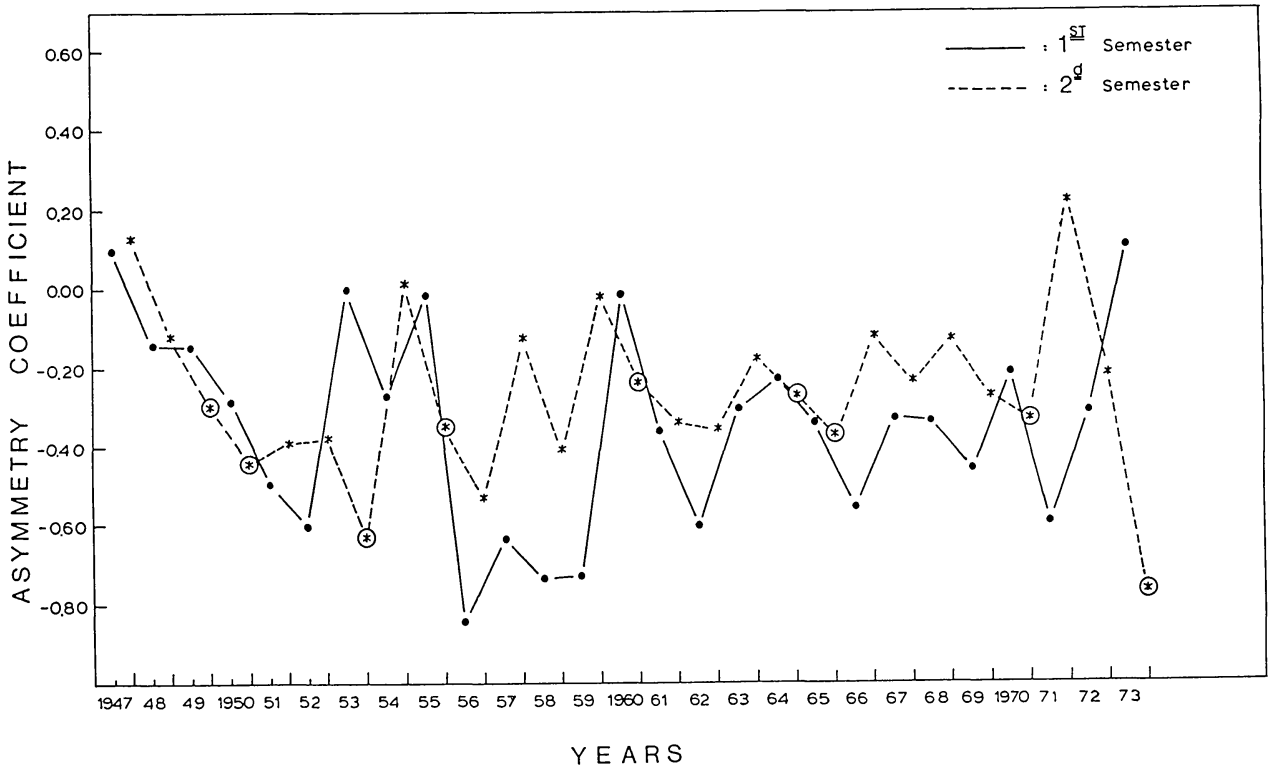

Fig. 6. Semi-annual variation of the E–W asymmetry coefficient of the green line intensity. Encircled points denote values of the second semester of a year which have failed to be greater than those of the first semester.

eighteen cases. After all, the aspect of an external influence (motion of the Sun towards the Apex) on the formation of longitudinal asymmetries of the solar activity and related phenomena like green line intensity, seems very possible. On the other hand, physical mechanisms associated with internal solar processings appear also promising in explaining longitudinal asymmetries. The idea of redistributions in the solar interior is supported by both observational and theoretical arguments like clustering of solar active regions in preferred longitudes which has been detected by Trellis (1960), Warwick (1965), Švestka (1968), Newkirk (1971) and non-axisymmetric solutions of the dynamo equations which have been computed by Krause (1971) and Roberts and Stix (1972).

Detailed measurements of the rotational rate and meridional drift of individual sunspots on a long series of spectroheliograms made by Ribes, Mein, and Mangeney (1985) have revealed that newly-born sunspots trace a roughly axisymmetric meridional circulation in the form of four zonal bands. This phenomenon could be very helpful in supporting large-scale motions at the solar photospheric level related to global convection and dynamo of the Sun. The interpretation of longitudinal asymmetries on the Sun exceeds the scope of this article but this subject deserves obviously an extensive analysis.

5. Solar Cycle Variations of the Green Line Intensity

Variations of the green line intensity with respect to the solar activity level are represented explicitly in Figure 7 where the mean yearly green line intensities for each solar quarter in the period 1944–1974 are depicted. From this figure, it is obvious that the NW quarter (continuous line) gives the highest intensity values within the time span 1949–1971, which is a 22-yr solar cycle starting two years after the maximum of the 11-yr cycle No. 18 and terminating two years after the maximum of the cycle No. 20. It is important to recall that 2–3 years after a solar maximum the solar magnetic field changes polarity and a new solar magnetic cycle starts (Wilcox and Scherrer, 1972). After the year 1971 the descending march of the NW variation and the ascending of the SW variation denotes clearly that the SW quarter gives the highest intensity values (broken line). It is very interesting to note that a relevant excess of the SW quarter can be also observed in the time span 1944–1948. Although the data of this period do not have sufficient statistical significance they appear to support the aspect that between successive 22-yr solar magnetic cycles the asymmetry between the north and the south hemisphere reverses its sign.

Finally, in the Figures 8 and 9 the mean polar distributions of the green line intensity is represented for the time periods 1944–1974 (Figure 8(a)), 1949–1971 (Figure 8(b)), 1944–1948 (Figure 9(a)), and 1972–1974 (Figure 9(b)). The mean polar distribution for the period 1944–1974 (Figure 8(a)) shows a butterfly feature the maximum intensity of which occurs within heliocentric sectors 10° far on both sides of the solar equator in the NW and SE solar quarters and 20° in the NE and SW quarters. In Figure 8(b), where the mean polar distribution of the green line intensity for the period 1949–1971 is depicted, the picture is similar with Figure 8(a) but the intensities of the NW quarter

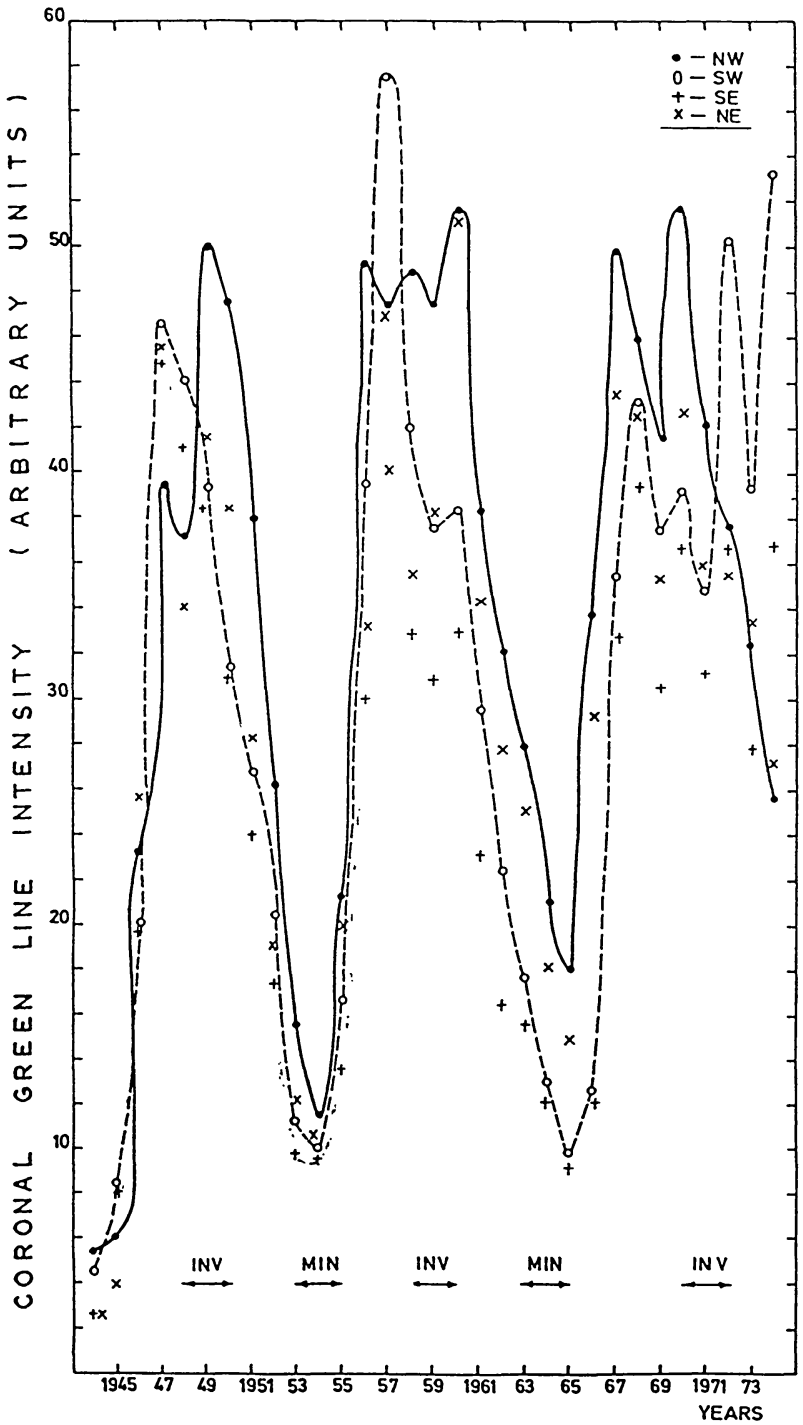

Fig. 7. Variations of the coronal green line intensity values of the northwest (●), southwest (○), southeast (+), and northeast (×) solar quarter in the time period 1944–1974. MIN and INV denote the epochs of minima and the solar magnetic field inversion, respectively.

in Figure 8(b) are higher than those of the corresponding quarter in Figure 8(a). In both Figures 8(a) and 8(b) the prevalence of the north on the south and the west on the east hemisphere is apparent. In Figure 9(a) we represent the less confident part of our data set which covers the part 1944–1948. In the data section of this article we have explained

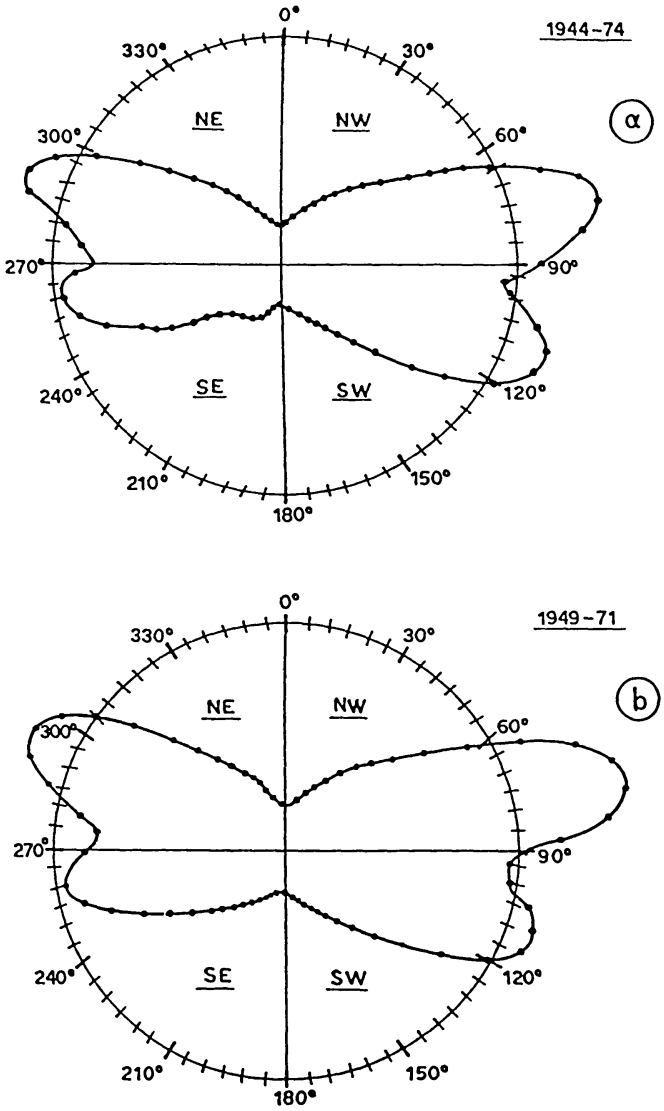

Fig. 8. Polar diagrams of the green line intensity distribution in heliospheric sectors 5° wide in the time periods 1944–1974 (upper panel), 1949–1971 (low panel). The NE, NW, SE, SW solar quarters are depicted orientating in this way the solar disc.

the reason why measurements of the years 1944 and 1945 do not offer sufficient statistical confidence. Nevertheless, a S–N asymmetry, especially in the west hemisphere, has been formed in Figure 9(a) which supports the aspect that a N–S asymmetry of a certain 22-yr solar magnetic cycle changes to a S–N one in the preceding and the following 22-yr cycle. The last argument is supported clearly by Figure 9(b) where the mean polar distribution in the period 1972–1974 is depicted. This period clearly belongs to the 22-yr cycle 1972–1994 and represents huge S–N and W–E asymmetries which mainly originate from the SW solar quarter.

In all cases, the maximum green line intensities appear in heliocentric sectors 10° far on both sides of the solar equator in the NW, SE solar quarters and 20° in the NE and SW quarters; namely, all the butterfly features of Figures 8 and 9 are 10° westward inclined in the solar coordinate system.

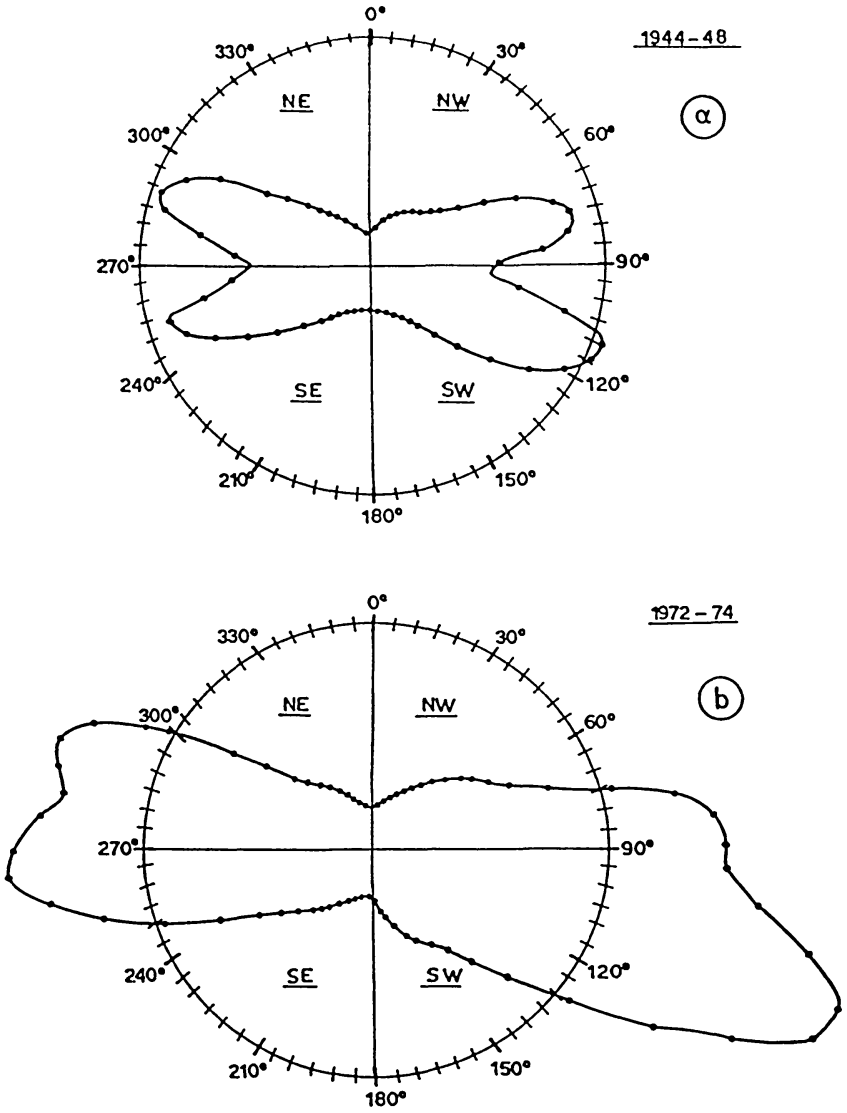

Fig. 9. Polar diagrams of the green line intensity distribution in heliospheric sectors 5° wide in the time periods 1944–1948 (upper panel), 1972–1974 (low panel). The NE, NW, SE, SW solar quarters are depicted orientating in this way the solar disc.

6. Conclusions

From the above analysis we can summarize the following:

(1) A N–S asymmetry of the green coronal line intensity has been confirmed in the time period 1949–1971. This time span corresponds to a 22-yr solar cycle which starts two years after the solar maximum of the No. 18 cycle – where the solar magnetic field inversion takes place – and terminates in the relevant epoch of inversion of the No. 20 cycle.

The N–S asymmetry seems to turn to a S–N one in periods they do not belong to the 22-yr cycle 1949–1971. Actually in the spans 1944–1948 and 1972–1974 the south solar hemisphere appears more active than the north.

The physical mechanism of a N–S or S–N asymmetry must be probably sought in

the different starting time of an 11-yr solar cycle in the two solar hemispheres. It has been mentioned that this starting time varies between the north and the south hemisphere from 1 to 3 years.

(2) A permanent and significant W–E asymmetry of the green line intensity has been detected in the time period 1944–1974. The physical mechanism of such an asymmetry is not very clearly understood, though both external and internal influences on the longitudinal distribution of the solar activity and related phenomena could contribute to the interpretation of this asymmetry. The motion of the Sun towards the Apex might apply an external influence on the longitudinal distribution of the solar activity while short-lived 'active' solar longitudes which are formed by temporal clustering of solar active centers may probably manifest an important internal influence which lead to the formation of an E–W asymmetry. In addition, a non-uniform solar rotation and cyclonic turbulence which can generate non-axisymmetric large-scale magnetic fields may also contribute significantly to a longitudinal asymmetry of the green line intensity (Stix, 1971).

(3) The combination of a N–S and a W–E asymmetry makes the NW solar quarter to appear as the most active of all in the 22-yr cycle 1949–1971.

In contrast, the combination of a S–N and W–E asymmetry proposes the SW quarter as the most active in the spans 1944–1948 and 1972–1974.

(4) A close covariance between the N–S asymmetries of the green line intensity and the sum of the maximum values of the solar magnetic field strength has been confirmed. This covariance argues for a narrow relation of the green line intensity to the solar activity.

(5) The study of the polar distribution of the green coronal line intensity, obtained within heliocentric sectors 5° wide, has located the maximum green line intensity of each solar quarter in sectors $\pm 10°$ far from the solar equator in the NW, SE solar quarters and $\pm 20°$ in the NE and SW quarters.

In the period 1949–1971 the maximum intensities of the north hemisphere are greater than those of the south. In contrast, in the periods 1944–1948, 1972–1974, the maximum intensities of the south hemisphere are greater than those of the north.

Acknowledgements

The authors express their gratitude to the colleagues of the Pic-du-Midi Observatory Drs Leroy and Noëns who provided us the data, as well as to the referee of this paper whose proper remarks improved its content significantly.

References

Antonucci, E.: 1974, *Solar Phys.* **34**, 471.
Bumba, V. and Howard, R.: 1969, *Solar Phys.* **7**, 28.
Cantú, A. M., Godoli, G., and Poletto, G.: 1970, *Astron. Astrophys.* **120**, L1.
Cuperman, S. and Sternlieb, A.: 1972, *Solar Phys.* **25**, 493.

Dollfus, A.: 1971, in C. J. Macris (ed.), *Physics of Solar Corona*, Astrophysics and Space Science Library, Vol. 27, p. 97.
Eddy, J. A.: 1976, *Science* **192**, 1189.
Howard, R.: 1974, *Solar Phys.* **38**, 59.
Jin, S. Z., Zhao, R. Y., and Fu, Q. J.: 1986, *Solar Phys.* **104**, 391.
Kendall, M. G.: 1948, *Rank Correlation Methods*, Hafner Publ. Co., New York.
Kendall, M. G. and Stuart, A.: 1966, *The Advanced Theory of Statistic*, Hafner Publ. Co., Vol. 2, New York.
Krause, F.: 1971, *Astron. Nachr.* **293**, 187.
Leroy, J. L and Noëns, J. C.: 1983, *Astron. Astrophys.* **120**, L1.
Leroy, J. L. and Trellis, M.: 1974, *Astron. Astrophys.* **35**, 283.
Letfus, V. and Růžičková-Topolová, B.: 1980, *Bull. Astron. Inst. Czechosl.* **31**, 232.
Maunder, A.: 1907, *Monthly Notices Roy. Astron. Soc.* **67**, 451.
Minnaert, M.: 1946, *Monthly Notices Roy. Astron. Soc.* **106**, 98.
Mitchell, J. M.: 1963, U.S. Weather Bureau, Washington D.C., p. 30.
Moussas, X., Papastamatiou, N., Rušin, V., and Rybanský, M.: 1983, *Solar Phys.* **84**, 71.
Newkirk, G.: 1971, in R. Howard (ed.), 'Solar Magnetic Fields', *IAU Symp.* **43**, 547.
Noëns, J. C. and Leroy, J. L.: 1981, *Solar Phys.* **73**, 81.
Pathak, P. N.: 1971, *Solar Phys.* **20**, 462.
Pathak, P. N.: 1972, *Solar Phys.* **25**, 439.
Ribes, L., Mein, P., and Mangeney, A.: 1985, *Nature* **318**, 170.
Roberts, P. H. and Stix, M.: 1972, *Astron. Astrophys.* **18**, 453.
Roy, J. R.: 1977, *Solar Phys.* **52**, 53.
Rozelot, J. P. and Fulconis, M.: 1983, *Solar Phys.* **84**, 77.
Rušin, V.: 1980, *Bull. Astron. Inst. Czechosl.* **31**, 9.
Růžičková-Topolová, B.: 1974, *Bull. Astron. Inst. Czechosl.* **25**, 345.
Stenflo, J. O.: 1972, *Solar Phys.* **23**, 307.
Stix, M.: 1971, *Astron. Astrophys.* **13**, 203.
Švestka, Z.: 1968, *Solar Phys.* **4**, 18.
Swinson, D. B., Koyama, H., and Saito, T.: 1986, *Solar Phys.* **106**, 35.
Stenflo, J. O.: 1972, *Solar Phys.* **23**, 307.
Trellis, M.: 1960, *Compt. Rend. Acad. Sci. Paris* **250**, 58.
Trellis, M.: 1967, *Astrophys. Letters* **1**, 57.
Tritakis, V.: 1984, *J. Geophys. Res.* **89**, No. A8, 6588.
Waldmeier, M.: 1971, *Solar Phys.* **20**, 332.
Waldmeier, M.: 1981, *Solar Phys.* **70**, 251.
Warwick, C. S.: 1965, *Astrophys. J.* **141**, 500.
Wilcox, J. M. and Scherrer, P. H.: 1972, *J. Geophys. Res.* **77**, 5385.
Xanthakis, J.: 1967, in J. Xanthakis (ed.), *Proceedings of a NATO Advanced Study Institute Conference*, Athens, September 1965, pp. 157.
Xanthakis, J., Petropoulos, B., and Mavromichalaki, H.: 1980, in CNES (ed.), *Soleil et Climat*, journées d'études internationales Toulouse, 30 Septembre–3 Octobre, 1980.
Xanthakis, J., Petropoulos, B. and Mavromichalaki, J.: 1981, *Solar Phys.* **76**, 181.